

## Autoresonance Cooling of Ions in an Electrostatic Ion Beam Trap

R. K. Gangwar,<sup>1</sup> K. Saha,<sup>1</sup> O. Heber,<sup>1</sup> M. L. Rappaport,<sup>2</sup> and D. Zajfman<sup>1</sup>

<sup>1</sup>*Department of Particle Physics and Astrophysics, Weizmann Institute of Science, Rehovot 7610001, Israel*

<sup>2</sup>*Physics Core Facilities, Weizmann Institute of Science, Rehovot 7610001, Israel*

(Received 13 November 2016; revised manuscript received 14 April 2017; published 8 September 2017)

Autoresonance (AR) cooling of a bunch of ions oscillating inside an electrostatic ion beam trap is demonstrated for the first time. The relatively wide initial longitudinal velocity distribution is reduced by at least an order of magnitude using AR acceleration and ramping forces. The hot ions escaping the bunch are not lost from the system but continue to oscillate in the trap outside of the bunch and may be further cooled by successive AR processes. Ion-ion collisions inside the bunch close to the turning points in the trap's mirrors contribute to the thermalization of the ions. This cooling method can be applied to any mass and any charge.

DOI: 10.1103/PhysRevLett.119.103202

Cooling of ensembles of ions, atoms, and molecules is a basic requisite in many branches of physics, such as spectroscopy [1], fundamental quantum physics [2,3], quantum electrodynamics [4], and quantum computation [5]. Traps for atoms and for ions are common devices in which cooling is done; however, beams, whether of neutral particles or ions, are also essential for some applications, especially for merged beams where precise control of the kinetic energies of the two beams permits fine-tuning of their relative velocities [6,7]. Many cooling techniques are available, the most common among them being laser cooling [8], stochastic cooling [9], electron cooling [10], and evaporative cooling [11,12]. Here we report on the cooling of a bunch of ions inside an electrostatic ion beam trap (EIBT) by means of autoresonance (AR) and ion-ion collisions.

In the present Letter, we demonstrate a technique by which  $\Delta p/p$  in an EIBT can be significantly reduced by removing from the bunch ions that are at the edges of the momentum distribution,  $\Delta p$ , so that the distribution in the bunch narrows, albeit with fewer particles. At the same time, ion-ion interaction near the turning points in the mirrors serves to thermalize the distribution. This scheme appears to be analogous to evaporative cooling that has been successfully applied in various ion traps, such as an electron beam ion trap [13–15] and Penning traps [16], and also found to be very efficient in achieving Bose-Einstein condensation [12] in atom traps.

An EIBT traps ions that are constrained by purely electrostatic fields to oscillate along a line within a relatively compact volume [17]. Ions are trapped between two electrostatic mirrors with adjustable focusing, as in an optical resonator [18]. The trap is tuned so that all ions with a certain kinetic energy to charge ratio ( $E_k/q$ ) can be trapped, and, as in all purely electrostatic devices, the trapping is independent of the ion mass. Here,  $E_k$  is defined as the kinetic energy of the ion in the *field-free* region of the trap. Typically, an ion beam with an energy width of

1%–2% can be trapped in the EIBT. The energy spread determines the beam temperature, defined as the internal velocity distribution in the frame of reference moving with the average speed of the injected ions. For example, an ion beam having large  $E_k$  in the lab frame (a few keV or more) may be considered cold if the ions in the beam have a kinetic energy distribution  $\ll 1$  eV in the moving frame. This is similar to high energy storage rings in which electron coolers can cool ions down to  $\Delta p/p \sim 10^{-7}$ . In some cases, the cooling of the beam is so strong that a phase transition into a liquidlike or ordered ionic beam can accrue [19,20].

The ion oscillation dynamics in an EIBT can be described by the slip factor  $\eta = -(2E_k/f_{\text{osc}})df_{\text{osc}}/dE_k$ , where  $1/f_{\text{osc}}$  is the oscillation period of an ion with kinetic energy  $E_k$  in the trap. From the slip factor, one can relate the ion velocity to its frequency, as will be demonstrated below. Tuning of the EIBT mirrors' potential gradient can change the slip factor from positive values through zero to negative values [21]. When the slip factor is zero, a very interesting phenomenon happens: The oscillation frequency of an ion is nearly independent of its energy (like a harmonic oscillator to first order) but depends only on the square root of its mass. This characteristic is applied for isotope separation in radioactive beam facilities [22]. When the slip factor is positive, *slower* ions oscillate with higher frequency than faster ions. In that case, and if ion-ion collisions are introduced, a self-bunching phenomenon can be observed [23,24]. The ion-ion collisions operate so that ions with the same mass and similar kinetic energy stick together as long as the ion density criterion is fulfilled [24]. This was demonstrated in several experimental and theoretical works [25–27]. On the other hand, if the slip factor is negative, the faster the ions, the higher their oscillation frequency; if one starts with all ions concentrated in a narrow spatial distribution, after a few tens of oscillations, the narrow bunch diffuses so that the faster ions lead and the slower ones trail. Moreover, if one includes ion-ion

interaction, this effective phase-space rotation is done even faster in a process called enhanced diffusion. This enhanced diffusion phenomenon was also demonstrated and used for phase-space manipulation by controlled delta-kick cooling [28]. Here we want to tune the EIBT to have a negative slip factor as a way to slice off the tails of the phase-space distribution in order to have a narrower momentum (frequency) spread. The ion-ion collisions will be used to thermalize the ions in the bunch. EIBT simulations have demonstrated two unique characteristics [29]. The first is that ion-ion collisions take place very close to the turning points of the mirrors, when faster ions are reflected and slower ones are still approaching. The second is that the ion density at the turning points  $\rho_t$  can be up to  $\sim 10^3$  greater than in the field-free region of the trap ( $\rho_0$ ), depending on the focusing tuning [30]. The ratio between these two densities, taken from Ref. [30], is given by

$$\frac{\rho_t}{\rho_0} = \left(\frac{R_0}{R_t}\right)^2 \left(\frac{\Delta z_0}{\Delta z_t}\right) \quad (1)$$

where  $R$  is the bunch radius and  $\Delta z$  its length. It was found by simulation [30] that the radii squared can be compressed by more than 2 orders of magnitude compared to the field-free region by tuning the focusing electrode ( $V_z$ ) of the mirrors (Fig. 1). The longitudinal compression ( $\Delta z_t$ ) was found to be much less significant. A typical number of ions in a bunch is  $10^5 - 10^7$  with the density in the field-free region  $\sim 50 - 5000$  ions/mm<sup>3</sup>. Therefore, it is expected that ion-ion collisions will mainly take place at the turning points. The ion-ion collisions also couple the longitudinal motion with the transverse motion [31]. In order to both take a slice of the phase space and thermalize it, the sliced bunch of ions must be decoupled from the “hot” ions so that further collisions will take place only among the sliced ions. The way to do this is by adiabatic AR acceleration, as will be explained below.

AR is a common phenomenon in which periodic behavior of a nonlinear physical system can be phase locked to an external periodic driving force—on the condition that the driving force is adiabatic and exceeds a certain threshold. The phenomenon has been well studied

in many systems, from particle accelerators [32] to planetary science [33]. See Fajans and Friedland for a short review [34]. Specifically for ion traps, AR has been used for antihydrogen production in a Penning-Malmberg trap [35] and for mass spectrometry in an EIBT [36].

Recently, a theoretical work was published [37] on AR with electrons inside a static potential well. In this study, it was demonstrated that AR can accelerate charged particles located in a specific slice of the phase-space distribution while conserving its phase-space area. However, so far, no interaction between the charged particles was specifically included. It was claimed that this interaction can be included as a self-field in the equation of motion. A self-field was already included in the case of a positive slip factor in an EIBT [25]. Here we demonstrate experimentally that ion-ion interactions can actually *increase* the phase-space density (PSD) of such an accelerated slice.

The experimental setup employed in the present study consists of an EIBT (Fig. 1) with an Even-Lavie supersonic expansion ion source (located on a high voltage platform).  $\text{SF}_6^-$  ions (mass 146 amu) or  $\text{SF}_5^+$  ions (mass 127 amu) produced by the source are accelerated to kinetic energy  $E_k = 4.2$  keV. The ions are then focused and steered using an Einzel lens, electrostatic deflectors, and a chicane beam cleaner before entering the trap. The trap is the analog of an optical resonator, consisting of two identical electrostatic mirrors with focusing electrodes ( $V_z$ ). The ions are injected by lowering the voltage on one of the entrance mirror electrodes ( $V_P$  in Fig. 1) from  $V_{P2}$  to  $V_{P1}$  and then stored by rapidly raising  $V_P$  before the ions, which were reflected from the exit mirror, can escape [17]. Typical mirror potentials are  $V_{P2} = 5.75$  kV,  $V_{P1} = 2$  kV,  $V_1 = 6.5$  kV,  $V_2 = 4.875$  kV,  $V_3 = 3.25$  kV,  $V_4 = 1.625$  kV, and  $V_5 = 0$  kV, and the mirror Einzel-lens potential is  $V_z$ , which is varied. The overall voltage settings are set so that the trap operates in the dispersive mode, i.e., with a negative slip factor,  $\eta < 0$ . The actual value of  $V_{P1}$  during injection affects the initial trajectories of the ions within the trap and was exploited to vary the number of trapped ions.

In the present experiments, the ions are detected by a pickup located close to the center of the trap. The signal from the pickup is amplified by a charge-sensitive amplifier and recorded by a digitizer at a sampling rate of 2.5 or 1 MHz. The digitizer is triggered after the ions are already trapped in the EIBT, and the output of the charge-sensitive amplifier was recorded for many ion injection and trapping cycles. The linearity of the method was reported in a previous publication and found to hold over more than 5 orders of magnitude, well beyond what is needed in this work [38]. It was also shown that this method is equivalent to measuring directly the ions with a particle detector [39]. In the case of  $\text{SF}_6^-$ , the peak of the second harmonic ( $2f_{\text{osc}}$ ) of the distribution for the  $\text{SF}_6^-$  ions was measured to be  $\sim 174\,450$  Hz (open circles in Fig. 2). The second harmonic was used to be compatible with

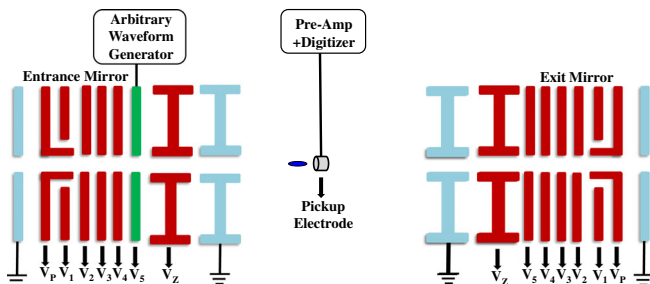


FIG. 1. A schematic drawing of the EIBT with pickup and bunching electrode (green).

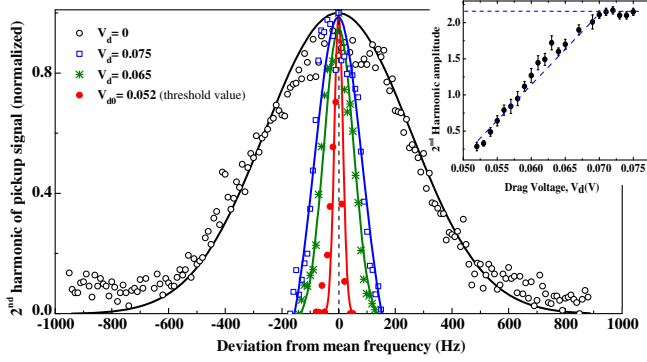


FIG. 2. Normalized distribution of the second harmonic of the oscillation frequency of  $\text{SF}_6^-$  plotted as the deviation from the mean frequency for different drag voltages  $V_d$ . The inset shows the actual peak height vs  $V_d$ . Note that, for  $V_d \geq 0.07$  V, the peak height is approximately constant.

previous work [40]. A Gaussian fit to the distribution gives a standard deviation  $\sigma \approx 250$  Hz, or  $\sigma/(2f_{\text{osc}}) = 0.00143$ , and  $f_{\text{osc}} = 87\,225$  Hz.

In order to demonstrate cooling in the trap, an AR force was applied to drag (adiabatically accelerate) the ions. The ions that do not fulfill the AR condition escape from the bunch, thus reducing the width of the energy distribution of the ions in the bunch. The undragged (residual) ions remain trapped with different energy. The force is produced by an arbitrary waveform generator (AWG) connected to electrode  $V_5$  on the entrance mirror (Fig. 1). The AWG is capable of sampling rates (SR) up to 100 MHz and of being triggered at any given time after the start of trapping. The duration  $T$  of the AWG drag-driving potential is defined by the number of sampling points,  $n$ , divided by the SR. The AWG is programmed to produce a chirped sine wave with four main parameters, viz., drag voltage  $V_d$ , initial frequency  $f_1$ , final frequency  $f_2$ , and  $T$ :

$$V_i = V_d \sin \left[ \left( \frac{2\pi(f_2 - f_1)i}{n} + 2\pi f_1 \right) i / \text{SR} \right] \quad (2)$$

where  $0 \leq i \leq n$  denotes the sampling point index of the AWG and  $n = T \text{ SR}$ . Typical operational parameters for  $\text{SF}_6^-$  are  $f_1 = 174\,200$  Hz,  $f_2 = 177\,000$  Hz, and  $T = 80$  ms. The ion frequency at the end of the chirp is  $f_2/2$ , because the frequencies used are  $\sim 2f_{\text{osc}}$ , which, as a by-product, also creates two bunches that oscillate simultaneously (in opposite directions) in the trap. With the above settings, it has been observed that the bunches can be accelerated to  $f_2/2$  only if  $V_d \geq V_{d0} = 0.0520 \pm 0.0005$  V, where  $V_{d0}$  is the AR threshold for the above settings. In this set of experiments,  $V_d$  was kept constant during the time  $T$ .

The frequency distribution was measured again immediately after the external force was stopped (AWG rf turned off), i.e., when only electrostatic forces were present in the trap. In Fig. 2, the new frequency distributions after AR

dragging are presented for  $V_d = V_{d0}$  and at two higher voltages. The standard deviation of the frequency distribution at the threshold,  $\sigma_0$ , is about 15 Hz, which is more than an order of magnitude smaller than before AR dragging. The results reflect a new frequency distribution, with ions in the two bunches that oscillate at  $f_2/2 \pm \sigma_0$  making  $177\,000/15$  half-revolutions in the trap before they return to their original phase-space distribution. One can define a synchronous particle as an ion that oscillates at exactly  $f_2/2$ . In the frame of reference of the synchronous particle, the ions at  $+\sigma_0$  ( $-\sigma_0$ ) make exactly one more (one less) half-oscillation than the synchronous particle before returning to the same point in phase space. Therefore, these ions traverse one trap effective length  $L/2$  ( $L$  is defined by the average ion velocity times the oscillation period) relative to the center of the bunch in  $1/15$  s. Since  $L/2 \sim 40$  cm, the velocity width is about 6 m/s, and the calculated temperature is well below 1 K.

The distribution width was found to be linearly dependent on  $V_d$  (more details in Supplemental Material [41]). The height of the distribution was also linearly dependent on  $V_d$  if  $V_d < 0.07$  V (inset in Fig. 2); above this value, the amplitude does not change, meaning that no more ions are lost from the center of the ion slice.

In order to conform to the common definition of cooling, one must look at the PSD [45]. If one defines the PSD as the number of ions divided by the phase-space area (in the longitudinal direction), then by measuring the velocity distribution, the longitudinal ( $X$ ) distribution, and the number of ions, one can calculate the PSD. We have measured the pulse widths and their frequency distribution with the pickup. The width in  $X$  is the pulse width divided by the ion velocity. The momentum width can be derived from the slip factor and the frequency width. The number of particles can be derived from the integral under the pulse. The results of these calculations as a function of  $V_d$  show a constant PSD, as predicted by Ref. [37]. This, however, neither proves nor disproves that thermalization has taken place, a necessary condition for phase-space cooling.

Therefore, further experiments were performed using a  $V_d$  that decreased linearly during the AR process as

$$V_d(i) = V_0 - (V_0 - V_T) \frac{i}{n} \quad (3)$$

where  $V_0$  is  $V_d$  at the beginning of the AR drive ( $i = 0$ ) and  $V_T$  is the value of  $V_d$  at the end of the AR drive ( $i = n$ ).  $V_d(i)$  replaces the constant  $V_d$  in Eq. (2).  $V_0$  was changed in small steps from  $V_T$  (constant  $V_d$ , as before) up to  $3V_T$ . In this set of experiments,  $\text{SF}_5^+$  ions (rather than  $\text{SF}_6^-$ ) were trapped to test settings for positively charged ions, and the only parameter that was changed in each measurement was  $V_0$ . The results are presented in Fig. 3. It can be seen that there is a maximum at  $\sim V_0/V_T = 2$ . The results indicate that more ions can be dragged to the same final position and velocity distribution just by controlling  $V_0$ . This was



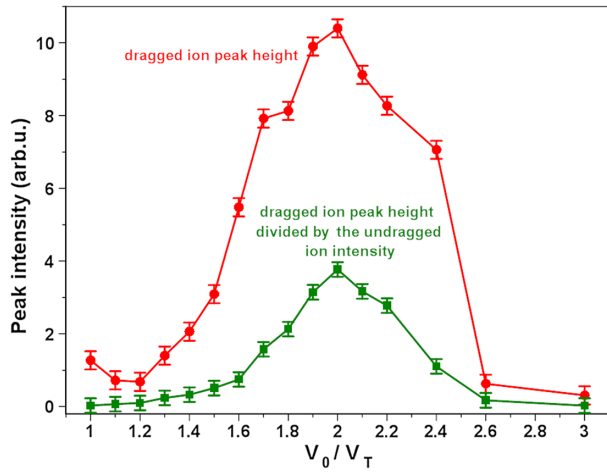


FIG. 3. Dragged bunch height of  $\text{SF}_5^+$  vs ratio between the initial and final values of  $V_d$ . The circles are the direct height measurements of the dragged ion intensity, while the squares are the same divided by the residual (not dragged) ions in the trap. The lines are a guide to the eye.

determined by measuring the frequency distribution of each bunch after the AR signal was stopped, which was found to be almost independent of  $V_0$  within the experimental error. Therefore, the measured heights of the frequency distribution shown in Fig. 3 represent the relative change in the PSD. Additionally, besides the dragged ions in the peak oscillating at  $f_2/2$  at the end of the chirp, there are the rest of the ions around the initial ion frequency ( $f_{\text{osc}}$ ). These ions can also be measured as an indicator of the number of ions in the trap (see Supplemental Material [41]). The square points in Fig. 3 represent the dragged peak height divided by the number of residual ions in the trap. Although it was shown that one can increase the PSD with different AR settings, it might very well happen with a single set of parameters of  $V_0$  and  $V_T$ , including  $V_0 = V_T$  and with a different number of trapped ions.

In order to check the PSD behavior of a single  $V_0$  and  $V_T$ , an additional set of experiments was performed in which  $V_{p1}$  was varied for the purpose of changing the number of trapped ions from zero to all the incident ions. In this set of experiments, a sine wave generator (SWG) was connected to electrode  $V_5$  along with the AWG so as to monitor independently the number of ions in the trap before and after the AR process. The two generators were operated at different times: The SWG was turned on 280 ms after the injection for  $\sim 30$  ms, while the AWG was turned on 320 ms after the injection for 80 ms. The digitizer began recording the pickup signal from the time the SWG was turned on and continued to record for 200 ms (more details in Supplemental Material [41]). Two main observables were measured: (i) the number of ions before AR, indicated by the peak intensity of the Fourier transform at the SWG frequency [46] during the first 10 ms of digitizing data, and (ii) the peak intensity of the Fourier transform of the ions after AR (from data recorded for 10 ms starting

immediately after AR, when only electrostatic fields are present). The results of the dragged ion intensity as a function of the number of ions in the trap are presented in Fig. 4. We have tried to fit the data with the polynomial  $ax^2 + bx + c$  ( $x$  is the injected ion intensity). The dashed line is a parabolic fit to the data with a single parameter ( $b = c = 0$ ). The mean squared error (mse) for the fit is 86.43. Using a single-parameter fit to a straight line ( $a = c = 0$ ) gave  $\text{mse} = 916$ . Similarly, using a two-parameter parabolic fit ( $c = 0$ ) gave  $\text{mse} = 85.98$ , which is a very small improvement compared to a single-parameter parabolic fit (Fig. 4). The error bars along the  $x$  axis indicate the standard deviation of the injected ion intensity after many consecutive injections for each  $V_{p1}$  setting. The increase in intensity with the square of the number of trapped ions is a clear indication that ion-ion collisions indeed occur and influence the PSD.

In summary, a new cooling technique has been demonstrated in an EIBT. The same technique may apply equally well to storage rings with focusing points for thermalization. The velocity distribution of the ions trapped in a bunch is modified by applying an autoresonance drag force that results in a significant reduction in the width (standard deviation) of the frequency distribution from about 250 to 15 Hz. The velocity distribution of ions within a bunch was reduced from an initial value of  $\sim 1000$  to  $\sim 6$  m/s by this technique. The number of ions in the dragged bunch was found to depend quadratically on the total number of ions in the trap, thus confirming the importance of ion-ion collisions (at the trap's turning points) to the thermalization of ions in the bunch. During the cooling process, most of the ions escaping from the bunch remain in the trap for further manipulation, e.g., successive cooling. If needed, it has been shown that the ions that are not within the bunch can be ejected from the beam by a kick-out electrode [47].

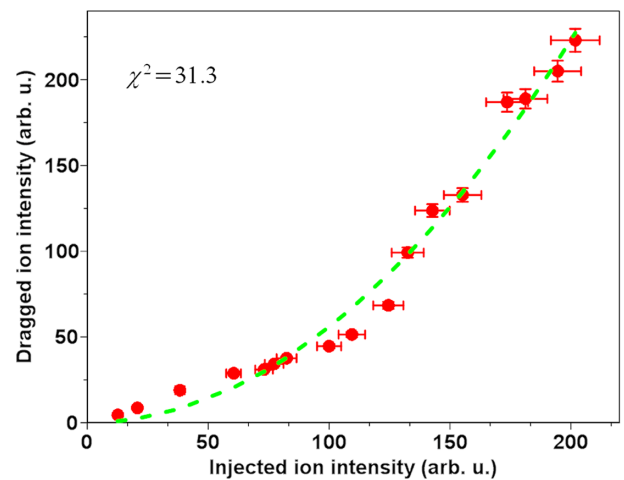


FIG. 4. Dragged ion intensity vs number of  $\text{SF}_5^+$  ions in the trap. The number of ions in the trap was measured using ion bunching before the AR process. The dashed line is a fit to a single-parameter parabola.

The results reported here are preliminary; it is expected that parameters such as chirp rate, rf waveform, final frequency, and mirror potentials can be optimized to cool the ions even further and/or faster.

We acknowledge the valuable comments and fruitful communications with Professors Andreas Wolf and Xavier Urbain, who were kind enough to critically review the manuscript. This research was supported by Benozio Endowment Fund for the Advancement of Science.

- 
- [1] T. R. Rizzo, J. A. Stearns, and O. V. Boyarkin, *Int. Rev. Phys. Chem.* **28**, 481 (2009).
  - [2] I. Bloch, J. Dalibard, and W. Zwerger, *Rev. Mod. Phys.* **80**, 885 (2008).
  - [3] *Annual Review of Cold Atoms, and Molecules*, edited by K. W. Madison, Y. Wang, A. M. Rey, and K. Bongs (World Scientific Singapore, 2013), Vol. 1.
  - [4] Y. Han, Z. Wang, and G. Guo, *Natl. Sci. Rev.* **1**, 91 (2014).
  - [5] R. Blatt and C. F. Roos, *Nat. Phys.* **8**, 277 (2012).
  - [6] A. B. Henson, S. Gersten, Y. Shagam, J. Narevicius, and E. Narevicius, *Science* **338**, 234 (2012).
  - [7] H. T. Schmidt *et al.*, *Rev. Sci. Instrum.* **84**, 055115 (2013).
  - [8] H. J. Metcalf and P. van der Straten, *Laser Cooling and Trapping* (Springer, New York, 1999).
  - [9] M. Blaskiewicz, J. M. Brennan, and F. Severino, *Phys. Rev. Lett.* **100**, 174802 (2008).
  - [10] M. Blaskiewicz, *Annu. Rev. Nucl. Part. Sci.* **64**, 299 (2014).
  - [11] D. Wineland and H. Dehmelt, *Bull. Am. Phys. Soc.* **20**, 637 (1975).
  - [12] W. Ketterle and N. J. Van Druten, *Adv. At. Mol. Opt. Phys.* **37**, 181 (1996).
  - [13] M. B. Schneider, M. A. Levine, C. L. Bennett, J. R. Henderson, D. A. Knapp, and R. E. Marrs, *AIP Conf. Proc.* **188**, 158 (1989).
  - [14] B. M. Penetrante, J. N. Bardsley, M. A. Levine, D. A. Knapp, and R. E. Marrs, *Phys. Rev. A* **43**, 4873 (1991).
  - [15] T. Kinugawa, F. J. Currell, and S. Ohtani, *Phys. Scr.* **2001**, 102 (2001).
  - [16] M. Hobein, A. Solders, M. Suhonen, Y. Liu, and R. Schuch, *Phys. Rev. Lett.* **106**, 013002 (2011).
  - [17] L. H. Andersen, O. Heber, and D. Zajfman, *J. Phys. B* **37**, R57 (2004).
  - [18] M. Dahan, R. Fishman, O. Heber, M. Rappaport, N. Altstein, D. Zajfman, and W. J. Van der Zande, *Rev. Sci. Instrum.* **69**, 76 (1998).
  - [19] M. Steck, K. Beckert, H. Eickhoff, B. Franzke, F. Nolden, H. Reich, B. Schlitt, and T. Winkler, *Phys. Rev. Lett.* **77**, 3803 (1996).
  - [20] A. Simonsson, H. Danared, A. Kallberg, and K.-G. Rensfelt, *Hyperfine Interact.* **146**, 209 (2003).
  - [21] H. B. Pedersen, D. Strasser, B. Amarant, O. Heber, M. L. Rappaport, and D. Zajfman, *Phys. Rev. A* **65**, 042704 (2002).
  - [22] R. N. Wolf, M. Eritt, G. Marx, and L. Schweikhard, *Hyperfine Interact.* **199**, 115 (2011).
  - [23] H. B. Pedersen, D. Strasser, S. Ring, O. Heber, M. L. Rappaport, Y. Rudich, I. Sagi, and D. Zajfman, *Phys. Rev. Lett.* **87**, 055001 (2001).
  - [24] M. W. Froese, M. Lange, S. Menk, M. Grieser, O. Heber, F. Laux, R. Repnow, T. Sieber, Y. Toker, R. von Hahn, A. Wolf, and K. Blaum, *New J. Phys.* **14**, 073010 (2012).
  - [25] D. Strasser, T. Geyer, H. B. Pedersen, O. Heber, S. Goldberg, B. Amarant, A. Diner, Y. Rudich, I. Sagi, M. Rappaport, D. J. Tannor, and D. Zajfman, *Phys. Rev. Lett.* **89**, 283204 (2002).
  - [26] T. Geyer and D. J. Tannor, *J. Phys. B* **37**, 73 (2004).
  - [27] T. Geyer and D. J. Tannor, *J. Phys. B* **38**, 3423 (2005).
  - [28] S. Goldberg, D. Strasser, O. Heber, M. L. Rappaport, A. Diner, and D. Zajfman, *Phys. Rev. A* **68**, 043410 (2003).
  - [29] O. Heber, N. Altstein, I. Ben-Itzhak, A. Diner, M. Rappaport, D. Strasser, Y. Toker, and D. Zajfman, *Nuclear Science Symposium Conference Record* (IEEE New York, 2004), Vols. 1–7, p. 1110.
  - [30] H. B. Pedersen, D. Strasser, O. Heber, M. L. Rappaport, and D. Zajfman, *Phys. Rev. A* **65**, 042703 (2002).
  - [31] D. Attia, D. Strasser, O. Heber, M. L. Rappaport, and D. Zajfman, *Nucl. Instrum. Methods Phys. Res., Sect. A* **547**, 279 (2005).
  - [32] E. M. McMillan, *Phys. Rev.* **68**, 143 (1945).
  - [33] L. Friedland, *Astrophys. J.* **547**, L75 (2001).
  - [34] J. Fajans and L. Friedland, *Am. J. Phys.* **69**, 1096 (2001).
  - [35] G. B. Andresen and the ALPHA Collaboration, *Phys. Rev. Lett.* **106**, 025002 (2011).
  - [36] A. V. Ermakov and B. J. Hinch, *J. Mass Spectrom.* **46**, 672 (2011).
  - [37] T. Armon and L. Friedland, *J. Plasma Phys.* **82**, 705820501 (2016).
  - [38] I. Rahinov, Y. Toker, O. Heber, D. Strasser, M. L. Rappaport, D. Schwalm, and D. Zajfman, *Rev. Sci. Instrum.* **83**, 033302 (2012).
  - [39] K. Saha, R. K. Gangwar, O. Heber, M. L. Rappaport, and D. Zajfman, *Rev. Sci. Instrum.* **87**, 113302 (2016).
  - [40] Y. Toker, D. Schwalm, L. H. Andersen, O. Heber, and D. Zajfman, *J. Instrum.* **9**, P04008 (2014).
  - [41] See Supplemental Material at <http://link.aps.org/supplemental/10.1103/PhysRevLett.119.103202> for Autoresonance threshold analysis and time dependency, which includes Refs. [42–44].
  - [42] L. Friedland, A. G. Shagalov, and S. V. Batalov, *Phys. Rev. E* **92**, 042924 (2015).
  - [43] H. Wiedemann, *Particle Accelerator Physics*, 3rd ed (Springer, Berlin, 2007).
  - [44] F. Tecker, *Proceedings of the CAS-CERN Accelerator School: Advanced Accelerator Physics*, edited by W. Herr, Report No. CERN-2014-009 (CERN, Geneva, 2014).
  - [45] A. M. Sessler, *COOL05*, edited by S. Nagaitsev and R. J. Pasquienelli (American Institute of Physics, New York, 2006).
  - [46] O. Heber, P. D. Witte, A. Diner, K. G. Bhushan, D. Strasser, Y. Toker, M. L. Rappaport, I. Ben-Itzhak, N. Altstein, D. Schwalm, A. Wolfand, and D. Zajfman, *Rev. Sci. Instrum.* **76**, 013104 (2005).
  - [47] Y. Toker, N. Altstein, O. Aviv, M. L. Rappaport, O. Heber, D. Schwalm, D. Strasser, and D. Zajfman, *J. Instrum.* **4**, P09001 (2009).